ChemBioChem

Research Article
doi.org/10.1002/cbic.202200183

Chemistry Europe
European Chemical Societies Publishing

www.chembiochem.org

VIP *Very Important Paper*

Assessment of Bioactivity-Modulating Pseudo-Ring Formation in Psilocin and Related Tryptamines

Claudius Lenz,[a] Sebastian Dörner,[a] Felix Trottmann,[b] Christian Hertweck,[b] Alexander Sherwood,[c] and Dirk Hoffmeister*[a]

Psilocybin (**1**) is the major alkaloid found in psychedelic mushrooms and acts as a prodrug to psilocin (**2**, 4-hydroxy-*N*,*N*-dimethyltryptamine), a potent psychedelic that exerts remarkable alteration of human consciousness. In contrast, the positional isomer bufotenin (**7**, 5-hydroxy-*N*,*N*-dimethyltryptamine) differs significantly in its reported pharmacology. A series of experiments was designed to explore chemical differences between **2** and **7** and specifically to test the hypothesis that the C-4 hydroxy group of **2** significantly influences the observed physical and chemical properties through pseudo-ring formation via an intramolecular hydrogen bond (IMHB). NMR spectroscopy, accompanied by quantum chemical calculations, was employed to compare hydrogen bond behavior in 4- and 5-hydroxylated tryptamines. The results provide evidence for a pseudo-ring in **2** and that sidechain/hydroxyl interactions in 4-hydroxytryptamines influence their oxidation kinetics. We conclude that the propensity to form IMHBs leads to a higher number of uncharged species that easily cross the blood-brain barrier, compared to **7** and other 5-hydroxytryptamines, which cannot form IMHBs. Our work helps understand a fundamental aspect of the pharmacology of **2** and should support efforts to introduce it (via the prodrug **1**) as an urgently needed therapeutic against major depressive disorder.

Introduction

Psilocybin (**1**, Figure 1) is the major natural product of the psychedelic fungi of the genus *Psilocybe* and other genera, the so-called magic mushrooms.[1] Central American natives have referred to these mushrooms as "Flesh of the Gods," and traditionally consumed them during divinatory ceremonies.[2] Upon ingestion, **1** undergoes dephosphorylation to yield the oxidation-sensitive psilocin (**2**, Figure 1), which causes both somatic and perceptual effects, including an altered sense of time as well as visual hallucinations with multi-colored fractals.[2] Equally remarkable are psychological effects that include profound introspect and potentially decreased depression when the material is administered under controlled facilitative conditions.[3] The relevance of **1** as a candidate prodrug to treat therapy-refractory depression and major depressive disorder is impressively underlined by clinical studies and has led to the breakthrough designation by the US Food and Drug Administration (FDA).[4]

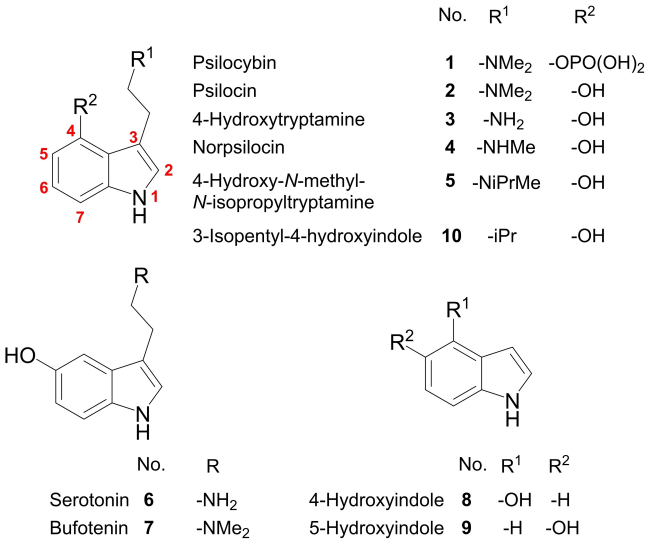

Figure 1. Chemical structures of natural and synthetic indole ethylamines and indoles.

The remarkable pharmacology of **2** and other indole ethylamines results in part from its interaction with serotonergic neurotransmission by binding to 5-HT receptors, primarily 5-HT_{2A}, with high affinity.[5] Serotonin (**6**, 5-hydroxytryptamine, 5-HT) is the endogenous ligand of the 5-HT receptors.[3] Although sharing very similar structural features, **2** and its 5-hydroxy isomer, bufotenin (**7**), markedly differ in their pharmacology. The toad-derived **7** does not show psychotropic effects when administered orally and in doses at which **2** is clearly psycho-

[a] C. Lenz, S. Dörner, Prof. Dr. D. Hoffmeister
Department Pharmaceutical Microbiology at the
Hans Knöll Institute, Friedrich-Schiller-Universität Jena
Beutenbergstrasse 11a, 07745 Jena (Germany)
E-mail: dirk.hoffmeister@leibniz-hki.de
[b] F. Trottmann, Prof. Dr. C. Hertweck
Department Biomolecular Chemistry
Leibniz Institute for Natural Product Research and Infection Biology
Hans Knöll Institute, Beutenbergstrasse 11a, 07745, Jena (Germany)
[c] A. Sherwood
The Usona Institute
2800 Woods Hollow Road, Madison, WI 53711 (USA)

Supporting information for this article is available on the WWW under https://doi.org/10.1002/cbic.202200183

active. As little as 3–4 mg of orally dosed **2** can induce measurable psychedelic effect in humans, whereas up to a 100 mg oral dose of **7** has been reported without a significant psychoactive effect.[5–7] Still, **7** tested in vitro has demonstrated potent agonist activity at the 5-HT_{2A} receptor.[8] The 5-HT compound **7**, like **6**, is suspected to have limited capacity to cross the blood-brain-barrier (BBB),[9] which is reflected by noticeable differences between **2** and **7** pertaining to their partitioning coefficients and in vivo distribution patterns (Figure S1, Table S1).[10,11]

Upon handling the 4- and 5-HT compounds, we observed differences in how rapidly they were (auto-)oxidized. The effects seemed to correlate with variations in the substitution pattern on the aminoethyl sidechain. We assumed that the structural features of the aminoethyl sidechain exerts influence on variable oxidation behavior via intra- or intermolecular O–H···N hydrogen bonds by lowering the oxidation potential of the phenolic hydroxy group.[12] This variable reactivity, taken collectively with the unique ability of **2** and other 4-HTs, but not 5-HTs, to readily cross the BBB, supports the notion of the postulated pseudo-ring formation in **2** through intramolecular interactions.[9,13] In contrast, a similar pseudo-ring formation is structurally impossible in **7** and other 5-HTs (Figure 2).

The presence of IMHB in **2** has been assumed, though no direct experimental evidence has ever been produced. Migliaccio et al. found significant differences in experimental pK_a values for the amino nitrogen (pK_a of **2**: 8.47, pK_a of **7**: 9.67), as well as for their partition coefficients, with **2** demonstrating more than an order of magnitude lower basicity by K_a and 1.8-fold greater lipid solubility independent of ionization differences (Table S1).[11] NMR experiments at 360 MHz indicated that **2** slightly favored a gauche conformer in solution suggesting a possible interaction between the 4-hydroxy and amino group. Direct evidence for the presence of an intramolecular hydrogen bond (IMHB), however, has not yet been obtained.

We address this gap in knowledge using modern NMR techniques and quantum chemical (QC) modeling, combined with kinetic examination of oxidation reactions involving specific structural variations of the substrate. We show direct evidence for intra- or intermolecular hydrogen bonds in 4- and 5-HTs, and how they possibly impact oxidative reactivity and molecular properties that relate to the remarkable pharmacology of **2**.

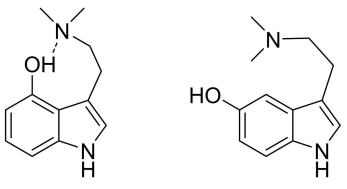

Psilocin (**2**) Bufotenin (**7**)

Figure 2. Comparison of the structures of **2** and **7** regarding pseudo-ring formation via intramolecular hydrogen bonds.

Results and Discussion

NMR spectroscopy to study hydroxytryptamine hydrogen bonds

IMHBs would plausibly explain the abovementioned features of 4-HTs. Therefore, we sought to identify such interactions by NMR analysis due to unique and therefore recognizable spectroscopic features.

NMR data also served to test predicted values. A recent report describes quantum chemical methods to obtain theoretical values for the Gibbs free energy of formation (ΔG) of both inter- and intramolecular hydrogen bonds, which were then validated by experimental data.[14] While this preceding study aimed at generating large databases of small-molecule IMHB strengths, we adopted the respective methods to study such interactions in greater detail in **2**, as well as to strategically selected related 4- and 5-HTs.

Equation (1) describes the approximate correlation of the OH chemical shift δ^{OH} (in ppm) with the free energy due to formation of a weak to moderately strong hydrogen bond (in kJ mol^{-1}) and was verified by IR spectrometric evaluation of IMHBs:[14–17]

$$\Delta G_{exp}^{IMHB} = -4.184 \cdot \left(\delta^{OH} - \delta_{Ref.}^{OH} + 0.4 \pm 0.2\right) \quad (1)$$

The reference value for the chemical shift was obtained from a related reference molecule unable to form the respective IMHB, i.e. **8** or **10** in the case of 4-HTs.

For experimental confirmation, we recorded ^{1}H NMR spectra of the compounds of interest in different solvents (Table 1), primarily acetone-d_6 and $CDCl_3$. Exchangeable protons were initially identified in the spectra of **2** and **7** by standard deuterium exchange experiments. As expected, two rapidly exchanging protons were present, corresponding to the OH and N1-H that were subsequently differentiated in a NOESY experiment (shown for **2** in Figure S2). Next, the spectral properties of the OH signals of **2–5** (4-HTs) and **7** (representing 5-HTs) were examined relative to the respective non-tryptamine reference compounds **8**, **9**, and **10** (Table 1). We observed chemical shifts across a range of nearly 9 ppm for the OH proton, with the most strongly deshielded OH protons found for **2** (and other 4-HTs).

The NMR spectra for **10** (Figures 1 and S3a-b) verified that C-3 indole alkylation only negligibly impacted the chemical shift of the 4-hydroxyl proton ($\Delta\delta = -0.02$ ppm from **8** to **10**). Compound **8**, whose OH signal appears as a sharp singlet at $\delta = 4.90$ ppm in $CDCl_3$ and at 8.18 ppm in acetone-d_6, was thereafter used as a non-IMHB-forming reference for 4-HTs. Similarly, the 5-hydroxy isomer **9**, shows OH shifts of $\delta =$ 4.42 ppm ($CDCl_3$) and 7.54 ppm (acetone-d_6). The large difference in OH shifts induced by the two solvents mainly reflects the propensity of acetone to act as a moderate H-bond acceptor, unlike chloroform.[18]

Hydrogen bonding increases the O–H bond length and correlates with considerable deshielding of the proton.[15,19] Therefore, a key observation for evaluation of potential IMHBs

Table 1. ^{1}H NMR chemical shifts of tryptamine hydroxyl and reference compounds (500 MHz, 300 K, 4.9 mM concentration), and experimentally derived free energy of formation of their respective (intramolecular) hydrogen bonds. Chemical shifts were referenced relative to residual protons present in $CDCl_3$ (δ = 7.24 ppm) and acetone-d_6 (δ = 2.05 ppm) or to the methyl signal of MeOH (δ = 3.31 ppm).

Compound	Solvent	δ^{OH} [ppm]	$\Delta\delta^{OH}$ from ref. [ppm]	ΔG_{exp}^{IMHB} [$\pm$0.8 kJ mol^{-1}]
4-hydroxyindole **8**	$CDCl_3$	4.90		
	acetone-d_6	8.18		
	MeOH	9.08		
3-isopentyl-4-hydroxyindole **10**	acetone-d_6	8.16		
psilocin **2**	$CDCl_3$	13.23	8.33[a]	−36.5
	acetone-d_6	12.21	4.03[a]	−18.5
	MeOH	n.o.[b]		
4-hydroxy-tryptamine **3**	acetone-d_6	12.20	4.02[a]	−18.5
norpsilocin **4**	acetone-d_6	~12.2[c]	~4.0[a]	−18.4
4-hydroxy-*N*-methyl,*N*-isopropyl-tryptamine **5**	acetone-d_6	12.37	4.19[a]	−19.2
5-hydroxyindole **9**	$CDCl_3$	4.42		
	acetone-d_6	7.54		
bufotenin **7**	$CDCl_3$	~5.7[c,d]	~1.3[e]	−7.0[f]
	acetone-d_6	7.53	−0.01[e]	

[a] Reference compound: **8**. [b] Not observed. [c] Strong to extreme signal broadening observed. [d] Unknown effective concentration due to precipitation. [e] Reference compound: **9**. [f] Intramolecular hydrogen bonding structurally impossible, value likely reflects intermolecular associations.

in **2** was its strongly deshielded OH proton, indicated by signals at δ = 13.23 and δ = 12.21 in $CDCl_3$ and acetone-d_6, respectively. Furthermore, we concluded that its chemical shift is less solvent dependent in comparison to reference compound **8**, with $\Delta\delta$ between $CDCl_3$ and acetone-d_6 of 1.02 ppm versus 3.28 ppm for **2** compared to **8**.

The OH proton in **2** (as opposed to **8**) is also characterized by a broadened signal. This feature suggests a greater involvement in rapid dynamic exchange processes or conformational transformations.[20] In contrast, a major downfield shift was not observed with **7**. In acetone-d_6, its OH proton signal (δ = 7.53 ppm) has a near-identical shift value as its reference **9** (δ = 7.54 ppm), indicating similar OH bonding states for these two compounds. $CDCl_3$ is an unfavorable solvent for a compound as polar as **7**. When **7** was solved in $CDCl_3$, a minor downfield shift ($\Delta\delta$ = 1.3 ppm) between **9** and **7**, accompanied by extreme broadening of the OH signal is found. It does however not compare to the severe downfield shifting from **8** to **2** in this particular solvent ($\Delta\delta$ = 8.33 ppm). Taken together, these findings suggest that the aminoethyl sidechain strongly interacts with the OH bond in **2**, but not in **7**.

IMHB formation should result in OH shifts that are less affected by concentration and temperature[21,22] due to IMHBs being independent from other analyte molecules and the thermally affected motions of the solvent molecules, respectively. Therefore, we investigated changes in hydroxyl proton signals as a function of these parameters. While both **8** and **9** show comparably small, yet modestly increasing slopes of δ^{OH} vs. analyte concentration, δ^{OH} of **7** is about eight-fold more affected than δ^{OH} of the former (Figure 3A). Conversely, δ^{OH} in **2** was also found less sensitive to varying concentrations, compared to **7** (Figures 3A and B). Its response was quantitatively comparable to **8** and **9**. Compound **2** appears to behave similarly to a compound that is incapable of inter-molecular interactions, suggesting predominant intra-molecular interactions. Dissimilar to the other compounds, however, some minor concentration-dependent molecular features of **2** seemed to approach saturation, as the impact on the OH signal appeared to be less pronounced or absent at the tested higher concentrations. Most noticeably, the OH signal of **2** does not further broaden between 9.8 and 24.5 mM (Figure 3B). These

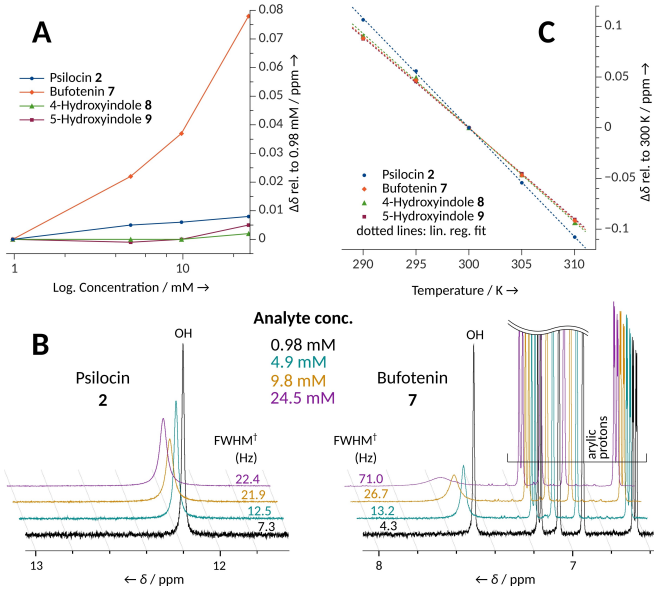

Figure 3. A) Logarithmic display of concentration-dependent hydroxyl proton chemical shift in **2**, **7**, **8**, and **9** (500 MHz, acetone-d_6, 300 K). Values are shown as differences to the shift values of the signal recorded at a concentration of 0.98 mM (δ_H = 12.20 (**2**), 7.51 (**7**), 8.18 (**8**), and 7.54 ppm (**9**), respectively). B) Overlaid portions of ^{1}H NMR spectra of **2** and **7**, recorded at different concentrations. The signal intensity of each spectrum was scaled to adjust aromatic proton signals to equal intensities. C) Temperature dependence of the same signal/compounds at a concentration of 4.9 mM. Values are shown as differences to the shift values of the signal at 300 K. Temperature coefficients were obtained by linear regression (see Table 2). † : Full width at half maximum (FWHM) of the respective OH signal.

observations corroborate that hydroxy groups in **2** are predominantly bound *intra*molecularly to the tertiary amine, which would be largely independent of concentration. Conversely, compound **7** lacks the ability to adopt a conformation capable of intramolecular interaction between the amine and hydroxyl proton and is, therefore, more prone to form *inter*molecular clusters (e.g., chains or dimers) by repeating phenol-amine interactions. With increasing concentration, the entropic cost of such clustering decreases, hence more and more hydroxylic protons become involved. In summary, concentration-dependent behavior of both OH signal shift and broadening with **7** reflected its propensity toward intermolecular interactions in solution (Figure 3A and B). Conversely, the OH signals for **2** are largely unaffected by changes in concentration, supporting the model that its proton was participating in an *intra*molecular interaction.

^{1}H shifts of IMHB forming hydroxy groups are usually less temperature-dependent than those in intermolecular clusters as they are less affected by the thermal motion of solvent and analyte molecules. This correlation was mainly studied for the chemically different and weaker IMHB interactions of e.g., polysaccharides[22] and peptides.[23] We observed a distinctly negative coefficient of −10.8 ppb/K for $d\delta^{OH}/dT$ in **2**, whereas **7**, **8** and **9** show values of around only −9 ppb/K (Figure 3C, Table 2). However, it is known from IMHB-forming terminal diamides, that interpretation of temperature-dependence becomes more complex with more flexible moieties involved in IMHB formation.[24] Importantly, the same study argues that pronounced proton deshielding (i.e., IMHB engagement) upon temperature decrease indicated a strong enthalpic benefit of a specific IMHB formation. Primarily when the geometric strains of the resulting pseudo-ring are minimal, this effect seems to overcompensate the decreased dependence on temperature due to excluded thermal motion.[24] Analogously, we assume that geometric requirements for IMHB formation (e.g., a near-linear O–H–N bond angle, later confirmed by QC modelling, Table S2) are well met in **2**, besides strong hydrogen bond donor and acceptor features.

To exclude the entropically unlikely possibility that the observed characteristics of δ^{OH} in **2** were caused by any unexpectedly strong *inter*molecular interaction from cluster formation in solution, diffusion-ordered ^{1}H NMR spectra (DOSY, acetone-d_6) for **2** and **7** (Figure 4) were compared.

We found similar diffusion coefficients (logD) for **2** and **7**, with the latter being less diffusive by about 0.4 log m^2 s^{-1} (value derived from arylic proton signals). This observation implied that **2** was slightly more compact in solution than **7**, consistent with **2** remaining monomeric, rather than forming larger clusters.

Table 2. Temperature coefficients of hydroxyl proton signals in **2**, **7**, **8**, and **9** in acetone-d_6 at a concentration of 4.9 mM.

Compound	δ^{OH} [ppm] at 300 K	$d\delta^{OH}/dT$ [ppb/K]	R^2 of $d\delta^{OH}/dT$
psilocin **2**	12.205	−10.8	0.9998
bufotenin **7**	7.532	−9.1	0.9996
4-hydroxyindole **8**	8.183	−9.3	0.9993
5-hydroxyindole **9**	7.537	−8.9	0.9998

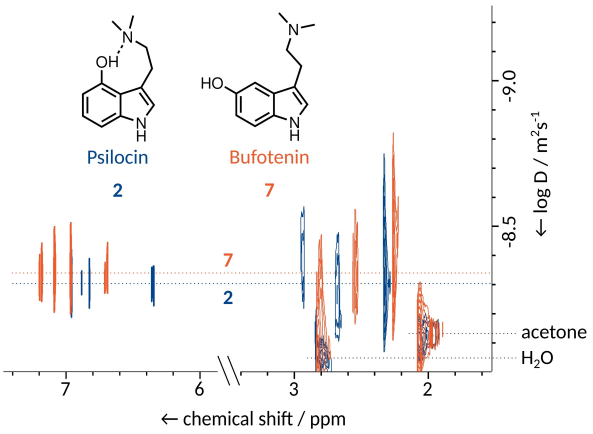

Figure 4. Overlaid ^{1}H DOSY spectra of **2** (blue) and **7** (ochre). 500 MHz, acetone-d_6, 4.9 mM concentration.

With regard to IMHB formation, our findings suggested that all simple 4-HTs demonstrated similar properties with observation of the hydroxyl proton by NMR (Table 1). Typically, hydrogen bond interactions within and between the analyte molecules decreased with increasing solvent polarity from $CDCl_3$ to acetone-d_6. When **2** was measured in the more polar MeOH (spiked with 5% MeOH-d_4), the OH proton signal did not appear (Figure S4). In comparison, **8** produced an OH signal in this solvent (9.08 ppm). Since major H/D-exchange does not occur under these conditions, this could indicate that in MeOH, the molecules of **2** may be involved in IMHBs as well, yet perhaps to some lesser extent than with the more apolar solvents. H_2O was tested (spiked with 5% D_2O) as well, but distinct OH signals were not observable in either **2** or in **8**. Hence, the applied NMR methods did not provide sufficient insight to allow for quantification of the strength of the potential IMHBs in MeOH or even H_2O.

Summarizing the observations from NMR experiments, we provide experimental evidence that **2** predominantly forms IMHBs between the phenolic 4-OH and the tertiary amine in apolar solvents leading to an apolar pseudo ring conformation and quantified the strength of this interaction in **2** by NMR spectroscopy (Table 1).

Further support for IMHB in **2** stems from infrared spectra, recorded in 1,2-dichloroethane. In the region between 3.200 cm^{-1} and 4.000 cm^{-1} only one band is observed for **2**, corresponding to the ν^{NH} (3.459 cm^{-1}) band (Figure S5). For **7**, two bands, corresponding to the free ν^{OH} (3.574 cm^{-1}) band and ν^{NH} (3.459 cm^{-1}) band are observed. Likewise, both **8** and **9** show two bands (ν^{NH} 3.460 cm^{-1} and ν^{OH} 3.566 cm^{-1}) in the typical range for ν^{OH} and ν^{NH} absorptions (Figure S5). Due to the equal intensity of the ν^{NH} (3.460 cm^{-1}) band in all four spectra, we excluded the possibility of a hydrogen bonded ν^{OH} band in **2** that has shifted to the same wavenumber as the ν^{NH} band. However, a broadened band (2.580 cm^{-1}) is observed in the spectrum of **2**, which is absent in the other compounds and

assigned as the hydrogen bonded ν^{OH} band. Due to the strong absorption of the solvent in parts of the respective signals, we re-recorded the IR spectrum of **2** in carbon tetrachloride. A band at 3.492 cm^{-1} and a broad band with a maximum at 2.577 cm^{-1} were observed and assigned to the ν^{NH} and the hydrogen bonded hydroxy group, respectively (Figure S5). The experimentally determined low wavenumber for the **2** hydroxy group is consistent with solid state IR data for **2**[25] (where the hydroxy group is intermolecularly bonded),[26] and literature data on comparable IMHBs, e.g., in 2,3,4,5-tetrachloro-6-((dimethylamino)methyl)phenol.[27] Therefore, IR data also support an IMHB, a property that is likely a key prerequisite for the ability of **2** to cross the BBB and, thus, for its psychotropic effects.

QC assessment of intramolecular hydrogen bond formation

To circumvent the above-mentioned NMR spectroscopy-related experimental limitations and provide further insight into potential IMHB properties of 4-HTs in aqueous environments, we performed quantum chemical modeling of the suspected IMHB. Theoretical values for the free energy change resulting from the formation of a hydrogen bond in solution can be obtained from QC calculations by the following Equation (2):[14]

$$\Delta G_{QC}^{HB} = \Delta E + \Delta G_{HO} + \Delta \delta G_{solv} \quad (2)$$

where E is total gas phase energy, G_{HO} is the sum of translational, rotational and vibrational free energy in the gas phase and δG_{solv} is free energy of solvation as obtained by calculations using solvent models,

Full geometry optimizations were performed both in gas phase and by utilizing solvent models, as well as harmonic oscillator calculations in gas phase. We used general-purpose dispersion-corrected density functional theory (B3LYP + D3(BJ)/def2-TZVP), known to be adequate for noncovalent tasks over a wide range of molecules.[28] In accordance with experimentally verified results,[14] the solvent model based on density (SMD) was used for implicit solvation. All differences 'Δ' in equation 2 span the reaction from the non-hydrogen-bonded molecules to those within the hydrogen-bonded complex. In the case of IMHBs, a suitable 'open' conformer represents the non-hydrogen-bonded state. Since the choice of the exact open form conformer is critical,[29] we initially performed a comparative conformational analysis by geometry optimization of individual conformers. The IMHB conformer of **2** (Figure 5A, species I) showed a significantly lower steric gas-phase energy than all non-IMHB conformers (31.96 kJ mol^{-1} lower than the second lowest conformer, Table S3). As per nomenclature of tryptamine conformers,[30] this global minimum conformation has the designation OH_{py}-E_{Gph}-N_{in}. For the reference 'open-form', two conformers were considered to theoretically assess the IMHB strength. The first one (Figure 5B, species II), referred to as OH_{ph}-E_{Gph}-N_{in} is derived from the closed conformation by simple rotation around the C–O bond. Among all 'open'-conformers, it showed the highest similarities with the IMHB conformer, and its generation does not involve major conformational changes. These features have been found to be essential for reference models in IMHB calculations.[14,29] Also, we expected OH_{ph}-E_{Gph}-N_{in} to provide calculation results that are in better agreement with NMR or IR spectroscopy data, which do not reflect e.g., the energetic benefits by full relaxation of the sidechain geometry, at least in solutions with one predominant conformer. Yet, of all non-IMHB conformations, the OH_{ph}-E_{Anti}-N_{ph} conformer (Figure 5C, species III) with its substituents standing *anti* at the ethylene showed the lowest energy in gas phase calculations as well as all calculated solvents (implicit modeling). Additionally, we found the vibrational change ΔG_{HO} for transferring the E_{Anti} sidechain conformer into either of the E_{Gph} conformers had a positive value of >6 kJ mol^{-1}. OH_{ph}-E_{Anti}-N_{in} was therefore assumed as major competitor towards the IMHB conformation OH_{py}-E_{Gph}-N_{in} under real-world conditions.

With these conformers, the free energy changes of IMHB formation $\Delta G^{HB}{}_{QC}$ were calculated (Table 3). With $CHCl_3$ as solvent, this theoretical value was in good agreement with the experimentally derived value (−35.1 versus −36.5 kJ mol^{-1}, respectively). However, upon modeled *in silico* solvation in acetone, the calculation result was strongly overbound (−18 kJ mol^{-1} error).

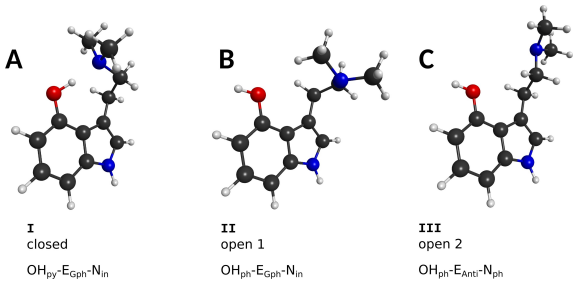

Figure 5. Conformations of **2**, as used in the QC calculations. The illustration shows geometries optimized through implicit modeling of $CHCl_3$. A) Pseudo-ring conformation with engaged IMHB (global lowest energy conformation). B) Non-IMHB conformation derived from A by turning its C–O bond, preserving the principal conformational situation of the side chain. C) Non-IMHB conformation including full relaxation of the side chain (lowest energy non-IMHB conformation, global second lowest energy conformation). Designation of conformers: OH_{py} – hydroxyl proton oriented towards pyrrole moiety; OH_{ph} – hydroxyl proton pointing in the direction of the phenyl ring; E_{Gph} – substituents of the side chain ethylene stand *gauche*, sidechain turned toward the phenyl moiety; E_{Anti} - substituents standing *anti* at the ethylene; N_{in} – amino-nitrogen lone pair pointing down/inwards to the ring system; N_{ph} – amino-nitrogen lone pair pointing toward phenyl ring.

Table 3. Calculated free energy changes (kJ mol^{-1}) for formation of the closed-IMHB conformer species I of **2** (implicit solvent modeling) and deviation from experimentally determined values (Table 1). Values in parentheses indicate the experimental error. For respective conformers I–III see Figure 5 and Figure S6a.

	Reference species	$CHCl_3$	Acetone	MeOH	H_2O
II	OH_{ph}-E_{Gph}-N_{in} (open 1)	−35.1 (+0.4)	−36.4 (−18.0)	−34.9	−27.3
III	OH_{ph}-E_{Anti}-N_{ph} (open 2)	−22.7	−23.7	−21.9	−13.6

As ΔE and ΔG_{HO} contributions are solvent-independent, this discrepancy necessarily reflects insufficient modeling of the solvation effects. Most likely, the implicit solvation model did not accurately reflect the contribution of the 'open-conformer' to form hydrogen bonds with the solvent, if the respective interaction is at least of moderate strength. With $CHCl_3$ as solvent, only weak interactions are expected with the phenolic group.

In contrast to $CHCl_3$, acetone can form O–H···O bonds, as indicated by the ^{1}H NMR OH signal of **8**, which experienced a strong downfield shift in acetone relative to its shift in $CHCl_3$ (Table 1). Similar deficient behavior of implicit solvent modeling was previously observed in a study computing the OH proton shifts of phenolic compounds in solvents of varying hydrogen bond formation capabilities.[31] To address this limitation, we adapted the model by treating a part of the solvent shell explicitly (hybrid solvation model, Table 4), which provided values consistent with the experimental hydrogen bond strength. With the hybrid solvation model, the calculated IMHB strength in acetone deviated by $-2.7\ kJ\,mol^{-1}$ in comparison to NMR result.

For this hybrid solvation model of the IMHB in acetone, we solely used the OH_{ph}-E_{gph}-N_{in} (open-) reference conformation of **2** (Figure S6b, species V), for the intended validation upon NMR derived data. We also used only one explicit solvent molecule, since acetone only forms one hydrogen bond (as an acceptor) with the OH group of **2**. The solvent molecule was placed in various positions around the OH and tryptamine sidechain region of the respective **2** conformers. Geometry optimization and free energy calculations of the resulting complexes were carried out as described for the implicit modeling. Harmonic oscillator calculations were limited, however, to the complex conformation of each type (open and closed), showing the lowest energy in solvent ($E+\delta G_{solv}$). This was considered adequate, as initial explorative calculations suggested that G_{HO} changes only marginally (typically $<2\ kJ\,mol^{-1}$) for equivalent sidechain conformations only differing by the position of the solvent molecule. Furthermore, ΔG_{HO} generally contributed the least to the overall IMHB strength.

For our eventual goal to evaluate IMHBs in **2** solved in H_2O, we formally used the same hybrid approach as described for acetone, but with the OH_{ph}-E_{Anti}-N_{ph} conformer as 'open' reference, providing the most conservative estimation approach to the IMHB strength, as suggested by implicit modeling results (Table 3). Also, we added up to three explicit H_2O molecules to account for the more complex positioning and possible hydrogen bonding interaction, arising from the small size and the multiple hydrogen bond acceptor and donor capabilities of this solvent.

Table 4. Calculated free energy changes ($kJ\ mol^{-1}$) for formation of the closed-IMHB conformer species IV (acetone), VI, VIII and X (one, two and three H_2O molecules, respectively) using explicit/implicit hybrid solvent modeling. Values in parentheses indicate the experimental error. For respective conformers IV–XI see Figure S6b-e.

Number of explicit solvent molecules	Acetone calc.	Ref.	H_2O calc.	Ref.
1	−21.2 (−2.7)	V	−16.3	VII
2			−16.6	IX
3			−22.8	XI

Surprisingly, the found IMHB strengths (−16.3 to $-22.8\ kJ\,mol^{-1}$) are larger than for the purely implicit solvent model, and also larger than in acetone, taking into consideration the different reference conformations in the chosen solvents. Even in a scenario of a substantially larger calculation error in H_2O than, e.g., in acetone, we assume the IMHB conformation of unprotonated **2** to be predominant in aqueous solutions. Its autocatalytic impact upon **2** oxidation is therefore expected for neutral to basic aqueous solutions.

Of note, in the case of three added water molecules, the geometry optimization in H_2O resulted in a proton transfer (Figure S6e, species X), as indicated by a shorter N–H than O–H bond length (1.09 vs. 1.49 Å, Table S2). This may be suggestive of a (zwitterionic) salt-bridge-like conformation for the 'closed' IMHB conformer in H_2O. Zwitterionic 'open'-conformations were not energetically favored in our calculations. However, as a potential intramolecular proton transfer in aqueous solutions of **2** is not in disagreement with our main hypotheses (i.e., the pseudo-ring-structure, BBB passage and oxidation speed modulation), we leave this question to future research.

The lower pK_a at the amine of **2** vs. **7** may result from a substantial OH···N stabilization in neutral **2**, which favors deprotonation. However, a notable, yet weaker antagonistic effect by intramolecular stabilization in N-protonated **2** (NH^+···OH-type) seems to exist, as suggested by additional supporting calculations (Supporting Information). Based on lowest energy conformers of either protonation state of **2** and **7** (i.e., both IMHB types found in **2**, Figure S6f), the difference of deprotonation free energies ($\Delta\Delta G_{deprot}$) between **2** and **7** is approximately $-10.5\ kJ\,mol^{-1}$, which is close to the experimental value of $-7.0\ kJ\,mol^{-1}$ derived from the reported ΔpK_a of −1.2.[11]

Aminoethyl sidechain effect on oxidation kinetics of hydroxytryptamines

Based on the results of our IMHB assessment, we assumed that structural differences in the aminoethyl sidechain correlate with changes in the rate of hydroxytryptamine oxidation. Therefore, we monitored the oxidation kinetics of **2**–**5**, and **7**, compared to 3-unsubstituted hydroxyindoles **8** and **9** as controls. When oxidizing 4- and 5-HTs (e.g., **2** or **7**) by either Fe^{3+} or IO_4^- in H_2O and MeOH at room temperature, quantitative turnover typically occurred in seconds to minutes. Oxidation conditions were therefore optimized to allow for chromatographic reaction time-course analysis (Figure S7). Briefly, a solvent-dependent decrease in reaction velocity was observed ($H_2O > MeOH > EtOH > n$-PrOH). Likewise, an acidic pH (pH 3.4 and 5) strongly decelerated the reaction. Under optimized conditions, using NBu_4IO_4 and *n*-PrOH at a temperature of 50 °C enabled chromatographic monitoring of the oxidation reactions of the substrates (Scheme 1, Figure S8). Excess NEt_3 was added to keep the substrates deprotonated.

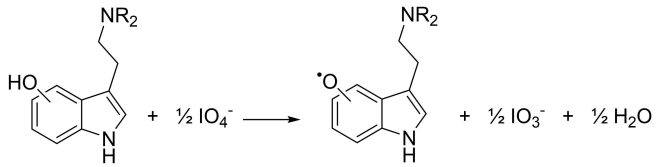

Scheme 1. Generic description of a typical initial hydroxytryptamine oxidation, i.e., dissociation of the OH bond and formation of respective radicals from the substrate, analogous to radical phenol oxidation.

The measurements demonstrated that the aminoethyl sidechain structure at C-3 correlated with oxidation reactivity when all other reaction parameters were held constant (Figure 6). Compared to the non-tryptamine 4-hydroxyindole **8**, **2** was oxidized about 5 times faster. When one or both *N*-methyl groups were absent, a dramatic acceleration of the oxidation was observed (25× with **3** and 20× with **4**). Conversely, if the amino group carried bulkier substituents, the assumed autocatalytic effect of the sidechain decreased or even reversed, as shown by the comparably slow oxidation of **5** (0.9 × as fast as for **8**).

Compared to the kinetics of **2** oxidation, the fast turnover of its 5-hydroxy isomer **7** was remarkable. However, relative to its respective reference **9** (which itself is oxidized about 3.6 times as fast as **8**) the oxidation of **7** was only 1.6 times accelerated. An enhanced stabilization of **7**-radicals at C-3, stabilized by the sidechain, may explain this observation, whereas radical stabilization at this position does not occur in 4-hydroxyindoles.

Arguably, *N*-oxide formation could also explain such patterns of substrate depletion kinetics. To rule out this potential confounding variable, product type examination by LC–MS under the kinetic study conditions with **2**, **3**, and **5** was conducted and did not indicate such reactivity. Post-column, no products due to assumed polymerization (**2** and **3**), or multiple peaks with *m/z* values suggesting oligomerization (**5**) were detected. Supra-noise level *m/z* values relating to *N*-oxides were not detected, neither in this study nor in previous reports upon oxidation of **2** or related hydroxytryptamines.[32]

As previously found for comparable phenol-amine compounds,[12] we conclude that the 4-hydroxytryptamine sidechains are involved in IMHB (O–H···N) formation and, thus, accelerate these phenol type oxidations of 4-HTs. These compounds oxidize autocatalytically, and this property is correlated with the *N*-substitution pattern of the sidechain. Since the general IMHB strength is not shifting significantly with various *N*-alkyl substituents, their steric demands may limit the accessibility of the phenolic OH to the oxidant. This eventually leads to (auto-)oxidation rates that make e.g. **2**, and even more **3** and **4**, unfavorable to store and handle in freebase solutions that are exposed to the atmosphere. However, bulkier *N*-substituents seem to represent soft protective groups, acting remotely through IMHB, that quench or even reverse this effect.

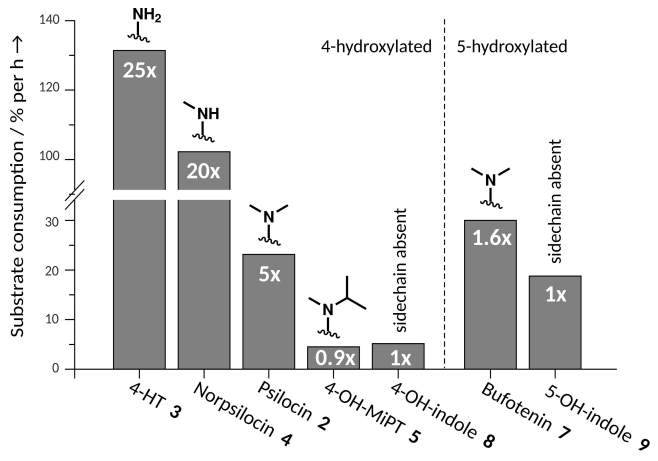

Figure 6. Comparative oxidation kinetics of 4- and 5-hydroxytryptamines with various sidechain *N*-substitution patterns (**2**-**5**, **7**) and their 3-unsubstituted parent compounds 4- and 5-hydroxyindole (**8** and **9**, respectively). HPLC-monitored oxidation of 500 μM substrate by 1.2 equivalents IO_4^- in *n*-PrOH at 50 °C. The acceleration of the reaction relative to the respective non-tryptamine references **8** and **9** are indicated. 4-OH-MiPT: 4-Hydroxy-*N*-methyl,*N*-isopropyltryptamine.

Conclusion

Our data on IMHB formation has both biosynthetic and pharmacological implications. With regard to biosynthesis, **1** assembly includes *N*,*N*-dimethylation,[33] which may help counter the oxidation lability of **2** to a degree the fungus can handle. Of note, the *Psilocybe* kinase PsiK of the **1** pathway fulfills a dual role as both a biosynthesis and a repair enzyme to rebuild **1** after spontaneous dephosphorylation to **2** inside an intact fungal cell.[4,34] This enzymatic protection system prevents the fungus from detrimental side-effects of **2** oxidation cascades, including radical coupling and protein precipitation by **2** oligomers.[32] However, this PsiK-mediated fail-safe requires that oxidation occurs slower than phosphorylation, which may not be the case with the primary amine **3**, compared to **2**. Previously, we hypothesized that **2** may play a role as a reactive and easily oxidizable monomer that readily oligomerizes into a potential defense compound.[4,32] The current results, presented here, support this view as the IMHB facilitates oxidation.

In the arena of pharmacology, our results on IMHB formation experimentally corroborate the long-standing hypothesis that **2** and other 4-HTs are potent orally available psychoactive compounds due to their unique intramolecular interactions. The propensity of **2** to form a pseudo-ring structure via an O–H···N bond has several implications.

Firstly, the energetic gain of the OH···N IMHB impedes both N-protonation and OH-deprotonation (Figure S9) as it is not equally countered by respective stabilizations in the ionized states. This plausibly explains the previously observed lower basicity of **2** vs. **7** (Table S1). Thus, considerably more uncharged species are present that partition from aqueous physiological environments into lipophilic membranes, such as the BBB.[11] Secondly, the molecule self-masks its most polar groups, resulting in an increased free energy of solvation in apolar media, which, again, leads to better partitioning. Thirdly, the pseudo-ring conformation may be the reason for the

comparably slow degradation of **2** by monoamine oxidase (MAO). Related compounds that cannot form IMHBs, such as the 5-HTs **6**[35–37] and **7**[9,11] are more prone to MAO-mediated degradation and generally too polar to cross the BBB. These features prevent exogenous 5-HTs to function as psychoactive compounds, although they serve as excellent ligands to 5-HT receptors in vitro.[6] However, non-hydroxylated tryptamines, such as *N*,*N*-dimethyltryptamine (DMT) and 5-methoxy-*N*,*N*-dimethyltryptamine are sufficiently apolar to cross the BBB, yet become rapidly degraded by MAO.[38] Consequently, they are orally inactive in the absence of MAO inhibitors.[39]

We conclude that our results help understand in greater detail the captivating pharmacology of **2**, a monomeric psychedelic natural compound that holds great promise as an urgently needed medication against major depressive disorder.

Acknowledgements

We thank A. Perner, H. Heinecke, and V. Hänsch (Leibniz Institute for Natural Product Research and Infection Biology, Hans-Knöll-Institute Jena) for recording HRMS and NMR spectra, and for support with chemical syntheses, respectively. We gratefully acknowledge R. Kargbo (Usona Institute, Madison) for providing reagents in support of these experiments. C.L. acknowledges a doctoral fellowship by the International Leibniz Research School (ILRS) for Microbial Interactions. This work was funded by the Deutsche Forschungsgemeinschaft (DFG, German Research Foundation) – Project-ID 239748522-SFB 1127 to C.H. and D.H., and by the Usona Institute (Madison, WI). Open Access funding enabled and organized by Projekt DEAL.

Conflict of Interest

The authors declare no conflict of interest.

Data Availability Statement

The data that support the findings of this study are available in the supplementary material of this article.

Keywords: bufotenin · hydrogen bonds · pharmacology · psilocybin · tryptamine

[1] A. Hofmann, R. Heim, A. Brack, H. Kobel, A. Frey, H. Ott, T. Petrzilka, F. Troxler, *Helv. Chim. Acta* **1959**, *42*, 1557–1572.
[2] J. Fricke, C. Lenz, J. Wick, F. Blei, D. Hoffmeister, *Chem. Eur. J.* **2019**, *25*, 897–903.
[3] a) F. Tyls, T. Palenicek, J. Horacek, *Eur. Neuropsychopharmacol.* **2014**, *24*, 342–356; b) R. B. Kargbo, *ACS Med. Chem. Lett.* **2020**, *11*, 399–402; c) D. E. Nichols, *J. Antibiot.* **2020**, *73*, 679–686.
[4] C. Lenz, A. Sherwood, R. Kargbo, D. Hoffmeister, *ChemPlusChem* **2021**, *86*, 28–35.
[5] W. J. Turner, S. Merlis, *AMA Arch. Neurol. Psychiatry* **1959**, *81*, 121–129.
[6] D. J. McKenna, D. B. Repke, L. Lo, S. J. Peroutka, *Neuropharmacology* **1990**, *29*, 193–198.
[7] J. Ott, *J. Psychoact. Drugs* **2001**, *33*, 403–407.
[8] B. L. Roth, M. S. Choudhary, N. Khan, A. Z. Uluer, *J. Pharmacol. Exp. Ther.* **1997**, *280*, 576–583.
[9] M. C. McBride, *J. Psychoact. Drugs* **2000**, *32*, 321–331.
[10] a) R. A. Glennon, P. K. Gessner, *J. Med. Chem.* **1979**, *22*, 428–432; b) F. Kalberer, W. Kreis, J. Rutschmann, *Biochem. Pharmacol.* **1962**, *11*, 261–269; c) R. W. Fuller, H. D. Snoddy, K. W. Perry, *Neuropharmacology* **1995**, *34*, 799–804.
[11] G. P. Migliaccio, T.-L. N. Shieh, S. R. Byrn, B. A. Hathaway, D. E. Nichols, *J. Med. Chem.* **1981**, *24*, 206–209.
[12] D. Kanamori, A. Furukawa, T. Okamura, H. Yamamoto, N. Ueyama, *Org. Biomol. Chem.* **2005**, *3*, 1453–1459.
[13] D. J. McKenna, G. H. N. Towers, *J. Psychoact. Drugs* **1984**, *16*, 347–358.
[14] C. A. Bauer, *J. Chem. Inf. Model.* **2019**, *59*, 3735–3743.
[15] I. Gränacher, *Helv. Phys. Acta* **1961**, *34*, 272–302.
[16] T. Schaefer, *J. Phys. Chem.* **1975**, *79*, 1888–1890.
[17] A. V. Afonin, A. V. Vashchenko, M. V. Sigalov, *Org. Biomol. Chem.* **2016**, *14*, 11199–11211.
[18] P. Gilli, L. Pretto, V. Bertolasi, G. Gilli, *Acc. Chem. Res.* **2009**, *42*, 33–44.
[19] F. Hibbert, J. Emsley, in *Advances in Physical Organic Chemistry* (Ed.: D. Bethell), Academic Press, New York, **1990**, pp. 255–379.
[20] J. I. Kaplan, G. Fraenkel, *NMR of Chemically Exchanging Systems*, Academic Press, New York, **1980**.
[21] R. J. Abraham, M. Mobli, *Magn. Reson. Chem.* **2007**, *45*, 865–877.
[22] B. R. Leeflang, J. F. G. Vliegenthart, L. M. J. Kroon-Batenburg, B. P. van Eijck, J. Kroon, *Carbohydr. Res.* **1992**, *230*, 41–61.
[23] T. Cierpicki, J. Otlewski, *J. Biomol. NMR* **2001**, *21*, 249–261.
[24] S. H. Gellman, G. P. Dado, G. B. Liang, B. R. Adams, *J. Am. Chem. Soc.* **1991**, *113*, 1164–1173.
[25] A. Hofmann, R. Heim, A. Brack, H. Kobel, A. Frey, H. Ott, T. Petrzilka, F. Troxler, *Helv. Chim. Acta* **1959**, *42*, 1557–1572.
[26] T. J. Petcher, H. P. Weber, *J. Chem. Soc. Perkin Trans. 2* **1974**, 946–948.
[27] a) A. Koll, P. Wolschann, *Chem. Monthly* **1999**, *130*, 983–1001; b) P. E. Hansen, J. Spanget-Larsen, *J. Mol. Struct.* **2016**, *1119*, 235–239.
[28] B. Brauer, M. K. Kesharwani, S. Kozuch, J. M. L. Martin, *Phys. Chem. Chem. Phys.* **2016**, *18*, 20905–20925.
[29] M. Jabłoński, *Chem. Phys.* **2010**, *376*, 76–83.
[30] J. R. Carney, T. S. Zwier, *J. Phys. Chem. A* **2000**, *104*, 8677–8688.
[31] M. G. Siskos, V. G. Kontogianni, C. G. Tsiafoulis, A. G. Tzakos, I. P. Gerothanassis, *Org. Biomol. Chem.* **2013**, *11*, 7400–7411.
[32] a) C. Lenz, S. Dörner, A. Sherwood, D. Hoffmeister, *Chem. Eur. J.* **2021**, *27*, 12166–12171; b) C. Lenz, J. Wick, D. Braga, M. García-Altares, G. Lackner, C. Hertweck, M. Gressler, D. Hoffmeister, *Angew. Chem. Int. Ed.* **2020**, *59*, 1450–1454; *Angew. Chem.* **2020**, *132*, 1466–1470.
[33] J. Fricke, F. Blei, D. Hoffmeister, *Angew. Chem. Int. Ed.* **2017**, *56*, 12352–12355; *Angew. Chem.* **2017**, *129*, 12524–12527.
[34] J. Fricke, R. Kargbo, L. Regestein, C. Lenz, G. Peschel, M. A. Rosenbaum, A. Sherwood, D. Hoffmeister, *Chem. Eur. J.* **2020**, *26*, 8281–8285.
[35] L. F. Mohammad-Zadeh, L. Moses, S. M. Gwaltney-Brant, *J. Vet. Pharmacol. Ther.* **2008**, *31*, 187–199.
[36] E. Afergan, H. Epstein, R. Dahan, N. Koroukhov, K. Rohekar, H. D. Danenberg, G. Golomb, *J. Controlled Release* **2008**, *132*, 84–90.
[37] S. Udenfriend, H. Weissbach, D. F. Bogdanski, *J. Biol. Chem.* **1957**, *224*, 803–810.
[38] S. A. Barker, J. A. Monti, S. T. Christian, *Biochem. Pharmacol.* **1980**, *29*, 1049–1057.
[39] L. P. Cameron, D. E. Olson, *ACS Chem. Neurosci.* **2018**, *9*, 2344–2357.

Manuscript received: April 1, 2022
Revised manuscript received: April 27, 2022
Accepted manuscript online: April 28, 2022
Version of record online: May 18, 2022